

Precision Orbit Determination for the Geosat Follow-On Satellites

Kelly Irish,* Kenn Gold,[†] George Born,[‡] Angela Reichert,* and Penina Axelrad[§]
University of Colorado, Boulder, Colorado 80120

The potential radial orbit accuracy of satellites in low Earth orbits has been investigated through simulation analysis and the reduced dynamic technique. Toward that end, a simulation interface has been developed so that the GIPSY OASIS II orbit determination software system may be used in simulation analyses. In simulation mode, orbits and measurement data are generated with a given set of models, after which the simulated data are processed with a different set of models. The results are compared to the simulated data, and the difference is due solely to modeling differences and data noise. By introducing model errors of appropriate size, realistic orbit error may be simulated. The simulation technique described has been applied to the GEOSAT Follow-On and TOPEX/Poseidon satellites. The results of the study, incorporating only six ground stations into the solution, show that radial orbit accuracy in the GEOSAT orbit will be approximately 4.3 cm rms. When the number of ground tracking stations was increased to 13 and the parameters for the reduced dynamic orbit determination technique were tuned, the radial error was reduced from 4.3 to 3.0 cm in the GEOSAT orbit and from 1.9 to 1.6 cm rms in the TOPEX/Poseidon orbit.

Introduction

A SATELLITE altimeter system does not directly measure the ocean surface height relative to a reference ellipsoid but uses a combination of radar altimetry and orbit determination to produce the measured sea height. Radial orbit error maps directly into sea surface height error. The radial accuracy of the TOPEX/Poseidon (T/P) precise orbits is estimated to be 2–3 cm rms, which allows monitoring of the Earth's sea surface topography with unprecedented accuracy.^{1,2} This accuracy has made possible the observation and study of many large- and small-scale phenomena that are of great importance to the overall objectives of the Earth Observing System (EOS). The continuation of the T/P high-precision sea surface height observations in future missions is a high priority to the global change and oceanographic communities. In addition, the GEOSAT Follow-On (GFO) missions will provide altimetry data in the GEOSAT exact repeat orbit (800-km altitude, 108-deg inclination). Ideally, the scientific community would like subcentimeter accuracy. However, because the GEOSAT orbit is at a much lower altitude than that of T/P (1340 km), the effects of atmospheric drag and gravity will make it difficult to attain comparable radial orbit accuracy.

The GEOSAT exact repeat orbit will be used by the GFO satellite launched in January 1998. The orbit options for GFO's follow on, GFO-2, are still under debate. One option is to continue the mission in the GEOSAT orbit, which would allow data continuity with the GEOSAT and GFO missions. Compared with the T/P orbit, it provides finer track spacing for coastal and mesoscale oceanography and better coverage of high-latitude oceanographic and glacial features. In addition, the simultaneous presence of GFO and GFO-2 in the same orbit for several years would allow unprecedented temporal sampling, which is particularly useful for reducing tidal aliasing in sea surface topography. Another option would be a joint NASA–Navy mission to combine GFO-2 and TOPEX/Poseidon Follow-On

(T/PFO) [also known as the EOS altimeter-radar (EOS ALT-R)]. This would require that the satellite, which would be nearly identical to the GFO satellite, fly in the higher 1340-km T/P orbit to meet the needs of both agencies by continuing the mission of T/P. A third option would be a joint NASA–Centre National d'Etudes Spatiales (CNES) mission also flying in the T/P orbit. Each of these missions will perform very accurate oceanographic altimetry from space and will carry global positioning system (GPS) receivers for tracking. Recently, NASA has chosen the third option, and T/PFO will be a joint NASA–CNES mission flying in the T/P orbit. However, we report the accuracy results for options one and two. The goals of all of these altimetric missions include monitoring various oceanographic features, such as currents, gyres, and eddies, and measuring global sea level.

Precise Orbit Determination

GIPSY-OASIS II is a high-precision software package developed by the Jet Propulsion Laboratory (JPL) for geodetic surveying and for orbit determination of low Earth orbiters (LEOs) using GPS.³ GOA II is used by JPL to process data from over 70 ground stations to produce daily GPS orbit solutions. Daily T/P orbits are produced using an 18-station subset of the more dense network.^{1,4} Three solution techniques are available for GPS-based orbit determination of Earth orbiters: 1) the dynamic technique, 2) the kinematic technique, and 3) the reduced dynamic technique (RDT). In the dynamic technique,⁵ models of the forces acting on the satellite are used to propagate the orbit solution from one epoch to the next. Tracking data are used to adjust dynamic model parameters, minimizing data residuals in a least-squares sense. The accuracy of orbits obtained with this method is directly dependent on the accuracy of the nominal force models, as well as the data accuracy. The kinematic technique relies solely on the geometry of the satellite measurements, and the accuracy of the solution is not dependent on dynamic modeling errors.⁵ However, for this technique to work, there must be excellent viewing geometry of the GPS satellites at every epoch of interest. The final method is the RDT.⁶ In this method, a converged solution is generated based on the most accurate dynamic models available. Once the converged dynamic solution has been generated, all dynamic model parameters are held fixed and additional accelerations are estimated in the radial, cross, and along-track directions. Thus, the RDT method is an optimal combination of the dynamic and kinematic techniques in the sense that it can provide the most accurate solution possible. The additional accelerations attempt to account for the error introduced by dynamic mismodeling and are modeled as first-order Gauss–Markov processes with associated steady-state sigmas and time constants. For the most

Received July 10, 1996; revision received Nov. 18, 1997; accepted for publication Nov. 25, 1997. Copyright © 1998 by the American Institute of Aeronautics and Astronautics, Inc. All rights reserved.

*Graduate Research Assistant, Colorado Center for Astrodynamics Research, Campus Box 431. Student Member AIAA.

[†]Professional Research Associate, Colorado Center for Astrodynamics Research, Campus Box 431. Member AIAA.

[‡]Professor and Director, Colorado Center for Astrodynamics Research, Campus Box 431. Fellow AIAA.

[§]Assistant Professor, Colorado Center for Astrodynamics Research, Campus Box 431. Member AIAA.

accurate solution, the RDT acceleration parameters must be adjusted so that their magnitudes accurately reflect expected dynamic modeling error. The RDT technique is used in this analysis for both the GEOSAT and T/P orbits, and tuning the magnitude of the RDT steady-state sigma is one focus of the study.

GOA II can be used for simulation and covariance analysis, as well as actual data processing. An interface was developed in which multiple simulations could be performed with simple user input, and the simulation capability of GOA II was enhanced to include several time-dependent effects. These included multipath error, stochastic drag error, and attitude error. GOA II was capable of dealing with these effects previously, but the new interface allowed their use with minimal effort. To perform in the simulation mode, GPS pseudorange and carrier phase measurements for both the LEO and ground station receivers are constructed using a series of truth files for the GPS and LEO satellite orbits, ground station coordinates, and other model inputs. These simulated measurements are then treated as though they were actual data. If these measurements were processed using the same models as were used to create them, the result would be a solution essentially identical to the truth orbit, assuming no data noise was applied.

This technique was used to ensure that the processing algorithms were working properly. However, if the simulated measurements are processed with slightly different models, the results will differ from the truth orbit. The differences will be completely due to the differences in models used. By differencing the truth orbit and the postprocessed solution arc, rms accuracy figures can be obtained. The simulation procedure shows how well the filter can estimate the original model parameters using erroneous models. Error sources that can be dealt with in the simulation include gravity model error, errors in the gravitational constant, atmospheric density, radiation pressure, ionospheric delay, tide models, spacecraft attitude, GPS satellite orbits, tracking station coordinates, tectonic plate motion, timing and polar motion, multipath reflection, spacecraft orientation, and data noise. The simulation package combines all of these error sources so that the analysis may be performed with only a few commands.

One benefit of using the interface to perform simulation analysis rather than covariance analysis is that it can be used to include time-varying error sources, which cannot be accomplished with covariance analysis.

Error Assumptions in the Precise Orbit Determination Analysis of GFO

There are two major concerns for accuracy of orbit determination for a continuing altimetry mission in the GEOSAT orbit rather than

the T/P orbit: 1) The atmospheric density and corresponding drag can be as much as a factor of two higher, and 2) orbit errors due to the geopotential are approximately a factor of three higher. However, previous studies have suggested that the gravity model should be tuned using GFO GPS tracking data obtained during solar minimum, thereby minimizing aliasing geopotential errors.⁷ Furthermore, the continuous, three-dimensional tracking provided by GPS is well equipped to remove unpredictable variations in the orbit caused by poorly modeled atmospheric drag.

The fidelity of an error analysis is directly dependent on the realism of the error models. The error models used in this study have been agreed upon by analysts at JPL; the Center for Space Research (CSR), University of Texas; and the Colorado Center for Astrodynamics Research, University of Colorado. The error sources used in this analysis are thought to be neither exceedingly optimistic nor overly pessimistic but are designed to be conservative to put a type of bound on the expected error. The error models fall into seven general categories: gravity-related errors, tides, Earth orientation errors, atmospheric drag, station-related errors, GPS measurement errors, and GPS orbit errors. These error sources are summarized in Table 1.

Specifics of Simulation Runs

Each simulated data set consists of a 30-h arc of GPS data from six ground stations and the flight receiver. The ground stations were chosen to provide global simultaneous data with the flight receiver to eliminate the effects of selective availability and to provide differential GPS data at every point in the orbit. GPS ephemerides from May 1, 1994, were used in the simulation and consisted of the 24 operational GPS satellites in their actual configuration on that date. The filter analysis assumed a flight receiver capable of tracking 10 GPS satellites (GFO-2 configuration) and implemented a 10-deg elevation cutoff, unless otherwise stated. Filter runs also were completed assuming a receiver capable of tracking only five satellites (the original GFO configuration) at various elevation cutoff angles. (The GFO receiver will now be a Turbo-Star capable of tracking eight satellites simultaneously.) The GFO spacecraft was modeled as a 3 × 1 × 3 m³ box with yaw-steering attitude control to simulate the expected on-orbit behavior required to point the fixed solar array.

It was desirable to isolate the various error sources so that their individual contributions to the overall error budget could be determined. Consequently, simulations were completed in which error sources were introduced individually. Errors in the RDT technique are dominated by GPS measurement error and GPS satellite observation geometry. In other words, for a simulation with perfect data and good geometry, RDT can remove all of the dynamic model errors. For this reason, GPS data noise (from a Gaussian distribution with standard deviation of 5 mm in phase) was added to each simulated measurement set. Other simulations in which all potential error sources were modeled simultaneously were completed. It is expected that these runs are the most realistic reflection of the possible orbit accuracy. The rms accuracy from simulations of individual error sources yields results similar to that of a simulation in which the error sources are modeled simultaneously. Descriptions of the individual error sources follow.

Gravity Errors

Errors due to uncertainty in the Earth's gravity field were simulated by generating data with the joint gravity model 2 (JGM-2) gravity field and then processing the simulated data set with the Texas Earth Gravity (TEG)-2B gravity field. Both fields used a 50 × 50 set of gravity coefficients. The differences between the two fields are thought to be representative of the expected error level for an untuned JGM-2 model at GEOSAT altitude. JGM-2 was chosen to be consistent with the other studies of GFO orbit accuracy, even though the newer JGM-3 model was available. An error of 0.0012 km³/s² was also added to the gravity model (GM) coefficient of the JGM-2 field. Dynamic solution techniques yield a radial orbit error due to mismodeled gravity on the order of 7-cm rms for the GEOSAT orbit. The RDT solutions show that gravity error effects can be reduced to approximately 3.4-cm rms.

Table 1 Error models

Error source	Error value
Gravity	JGM-2 minus TEG-2B
GM	0.0012 km ³ /s ²
Ocean tides	3% error in K ₂ , CSR tide model
Solid-Earth tides	3% error in K ₂ , CSR tide model
Atmospheric drag	1) 50% error in drag coefficient at solar maximum 2) Density temporal model (DTM) minus DTM with a factor of two-step function in density over one-fourth of each orbit
GPS orbits	Actual GPS orbit errors from overlap portion of TOPEX solution, May 1, 1994, rms differences of 50 cm
Ground tracking sites	Three deep space network stations (fiducial): 0 cm in each component Three other stations (adjusted): 1 cm horizontal, 3 cm vertical
Tectonic plate velocity	5-mm/yr error
Timing/polar motion	1 ms ⁻¹ in five day values of [x _p , y _p , universal time 1 (UT1)]
Antenna field of view	10-deg elevation cutoff angle
Measurement noise	0.5 cm in carrier phase; 1.0 m in pseudorange
Radiation pressure	50% in reflectivity, albedo, emissivity
Spacecraft yaw	Sinusoidal yaw error, 1–2 deg per orbit
Multipath	JPL/Hajj multipath model ⁹

Atmospheric Drag

Atmospheric drag is expected to be a major source of error at GFO altitude, and this error is modeled in several ways. In the simplest approach, the value of the GFO drag coefficient (estimated once over the entire 30-h arc) was to simulate various levels of solar activity. For the lower limit, a 10% error in the drag coefficient and solar flux values corresponding to a solar minimum were processed and compared to values of perfect models. The RDT technique removed nearly all of this error. For the upper limit, a 50% error in the drag coefficient and the maximum solar flux values were used. The level thought to be most representative of expected error was a 30% error in the drag coefficient used with a maximum solar flux. This 30% error is used when all errors are considered simultaneously. Even at the higher error levels, the RDT technique reduces the drag error to a few millimeters in the radial component.

Additional drag studies were conducted, in which a once-per-revolution density perturbation was added to the nominal value to simulate unmodeled time-varying effects. For the first case, a step function model (Fig. 1) was substituted for the nominally sinusoidal density for one-quarter of each orbit. The size of this step function was approximately twice the value of the maximum nominal density. Twice the value of the maximum nominal density is a conservative estimate of the amplitude of unpredictable density fluctuations due to gravity waves and winds.⁸ The RDT results show that this error causes a 9-mm rms error in the radial direction (Fig. 2). When the density error was combined with a 50% error in drag coefficient and the measurements were corrupted by data noise, this value increased to 1.6-cm rms.

GPS Orbit Errors

GPS orbit errors for the simulation consisted of GPS orbit position error and errors introduced by rotation of the satellite state from Earth fixed to inertial coordinates, i.e., timing and polar motion. GPS

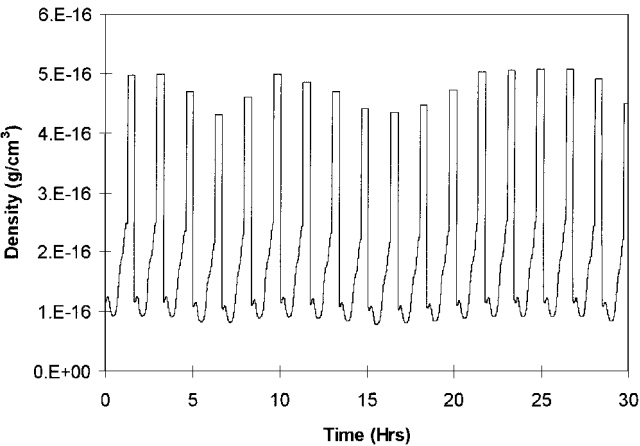


Fig. 1 Atmospheric density used for simulated drag error.

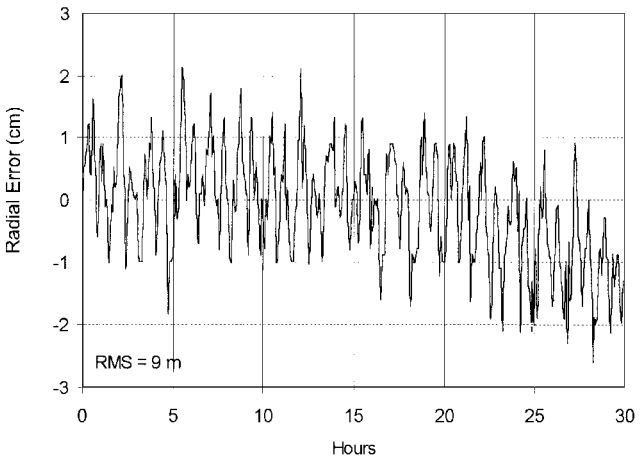


Fig. 2 Postfiltered GFO orbit compared to nominal (using Fig. 1 density profile).

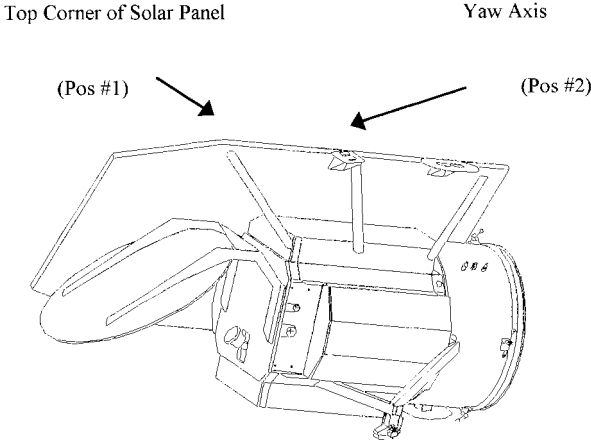


Fig. 3 GFO spacecraft with two potential GPS antenna locations indicated.

orbit error was created by differencing two JPL three-day GPS solution sets (with ~29 h of overlap) and adding these difference errors to the broadcast ephemeris states used in generating the data. The simulation did not estimate GPS orbits but used the perturbed GPS states as truth. The overlap rms GPS orbit difference was approximately 50 cm, radially, and the GPS orbit error introduced by timing and polar motion errors was on the order of 5 cm. The effect of GPS orbit error on GFO radial position was about 0.5-cm rms.

GPS Measurement Errors

In addition to Gaussian data noise, other error sources affect the GPS measurements. The phase center of the GPS antenna onboard GFO must be related to the spacecraft center of mass for orbit determination. Determining the position of the phase center of the antenna requires knowledge of the GFO orbit and attitude and the position of the GPS antenna relative to the center of mass of the spacecraft. Errors in the assumed spacecraft attitude affect the computed antenna phase center from the center of mass. Multipath contamination, in which GPS signals are reflected or diffracted by other spacecraft surfaces before reaching the antenna, can also be significant. Both of these error sources are affected by the placement of the antenna onboard the spacecraft. Two possible locations for the GPS antenna on GFO are shown in Fig. 3. The implications of either location are discussed in the following sections, which describe how each error source was modeled. The methods used to simulate the attitude and multipath error are significant new contributions.

Phase-Center Migration Induced by Attitude Error

Phase-center variations caused by yaw-attitude error due to eclipse entrance and exit, magnetic pole crossings, or other bias errors were simulated. The attitude-control algorithm used on GFO utilizes information from sun sensors and magnetometers to determine the spacecraft orientation. As the spacecraft passes through the Earth's shadow, the sun sensors lose sight of the sun, and the magnetic field is used instead to estimate yaw. The maximum length of the eclipse event is approximately 35 min.

This effect is modeled in the simulation analysis by first determining the occurrences of the umbral eclipse events with data from the GOA-II orbit integrator. Then a systematic yaw error is introduced into the simulation at entrance into the eclipse. In this evaluation, the yaw error introduced represents a worst-case scenario, where the added error is equal to 1 deg (1 + |sin(*f*)|) at the given time, where *f* is the true anomaly. Note that this worst-case error source was used for the runs in which all error sources were considered together. Quaternion sets representing the perturbed attitude of the spacecraft were used in the data generation step in GOA II. The data were then processed assuming unperturbed yaw.

If the GPS antenna is placed in the spacecraft body-fixed *x*-*y* plane, directly over the yaw axis (see Fig. 3) the effect of yaw error will be minimal. However, it was originally thought that it may be desirable to move the antenna to a location near the top of the solar panel to minimize multipath reflection. In this case, the antenna

would be approximately 1 m from the location of the yaw axis, and the phase center modeling would be more difficult, due to the yaw error. A secondary effect of this attitude orientation results from the changing center of mass of the spacecraft as fuel is consumed during the mission. Note that the yaw axis intersects the center of mass. If the antenna is placed directly above the prelaunch center of mass, at the end of the mission this location will be approximately 5 cm away from the yaw axis because the yaw axis goes through and moves with the center of mass. Thus, the end-of-life error is reduced if the antenna is placed on the yaw axis at the beginning of the flight, rather than at the edge of the solar panel. The results of the yaw-induced phase center error simulations are summarized in Table 2.

Multipath Error Simulation

The multipath environment was simulated for the GFO spacecraft using a multipath simulator developed at JPL.⁹ This simulator relies on geometrical optics for the main effect of multipath and utilizes the geometrical theory of diffraction, including diffraction from edges. A spacecraft body and its instruments can be modeled as conducting or dielectric flat surfaces, spheres, sections of spheres, cylinders, sections of cylinders, and conducting or dielectric surfaces. Both right- and left-hand circular polarized direct and reflected signals can be modeled, as well as specific antenna gain patterns. The simulator calculates the multipath contribution from each surface and GPS satellite pair and then combines the effects of all surfaces for both phase and pseudorange data at L1 and L2 frequencies. In the simulator, the GFO spacecraft was modeled as nine separate surfaces. Given the GPS position, the position of GFO, the orientation of GFO, and the measurement file, the multipath value for each GPS/GFO pair was determined and added to the measurement.

To confirm the errors predicted by the multipath simulator, an experiment was conducted with a GFO spacecraft mockup. A GPS antenna was placed on the mockup and was connected to a single-frequency GPS receiver. GPS phase errors were measured and compared with simulated data. The agreement was generally good in terms of magnitude, rms value, and frequency and is shown for one GPS satellite in Fig. 4. The high-frequency components of the observed multipath are due to receiver noise.

Table 2 Orbit error resulting from yaw-induced phase center error, end-of-life CG

Antenna location case	1 deg (1 + sin(<i>f</i>)) yaw error, mm			
	Radial track	Cross track	Along track	Three dimensional
Yaw axis	4.3	5.2	5.6	8.8
Top of panel	9.3	11.8	17.8	23.3

For the GFO precise orbit determination analysis, the predicted multipath delay was added to a simulated data file, which was then analyzed with GIPSY-OASIS II. If no other errors are added to the simulated data file, then the effect of multipath error can be determined. Three different antenna gain patterns were used in the simulation, with the phase center of the antenna placed in the two mentioned locations. Based on the simulation, it was determined that multipath on the GFO spacecraft has a small effect on phase observations.

The results for the orbit error due to multipath are shown in Table 3. In the orbit accuracy study, multipath was modeled for the two possible antenna locations already described and with three different antennas. The Tecom is the antenna used on the TOPEX mission, and the single-fed patch antennas will be used for GFO. The dual-fed patch was an additional possibility for use on GFO. If the GFO spacecraft is flown in the T/P orbit, the satellite configuration proposed for EOS ALT-R is similar to GFO and a GPS antenna mast may be employed as well. Therefore, the multipath effects for EOS ALT-R would be no worse than for GFO, and we have conservatively assumed that they will be the same.

Other Non-Gravity-Related Error Sources

Dynamic modeling errors are present due to various radiation effects including solar radiation pressure, Earth albedo, reflection, and emissivity. In GOA-II, scale factors are applied to accelerations from solar and Earth radiation parameters, and a simple attitude control law determines the surface area projected toward the various radiation sources. Errors in the radiation models were simulated by perturbing the values of these scaling coefficients between the data generation and processing steps. Thus, a reference orbit is generated, and this orbit is perturbed by changing the scaling coefficients. The perturbed reference orbit is used to make a measurement file. The measurement file is processed with the original unperturbed orbit file to determine the effect of using a slightly erroneous radiation model. In this simulation, a scaling error of 50% was investigated.

Several error sources relating to GPS ground stations were simulated, including station location errors, *K*₂ solid Earth tides, and *K*₂ ocean tides. The *K*₂ variations were introduced for consistency with the error study completed at the University of Texas.⁷ The contribution of station location errors was estimated by randomly perturbing the station coordinates so that they are slightly different from the coordinates used to generate the reference or truth data. In the six-station scenario, three stations were not perturbed, whereas the horizontal components of the others were given 1-cm errors, with the vertical components at 3 cm. This method of introducing measurement error has been demonstrated by JPL, and by convention it is done the same way here. The *K*₂ coefficients in the solid Earth and ocean tide models were perturbed by 3%. Tectonic plate

Table 3 Radial orbit error due to multipath in the GFO orbit: 10-satellite case

Antenna	Yaw axis				Top of panel			
	Radial, mm	Cross, mm	Along, mm	Three dimensional, mm	Radial, mm	Cross, mm	Along, mm	Three dimensional, mm
Tecom	2.7	2.9	2.8	4.9	2.95	3.7	3.9	6.1
Dual-fed patch	2.1	3.1	2.4	4.5	2.8	3.4	3.55	5.67
Single-fed patch	2.3	3.3	3.0	5.0	3.0	3.6	4.0	6.2

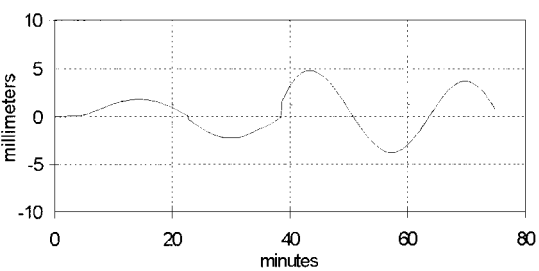
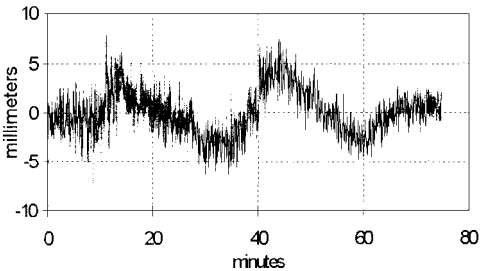


Fig. 4 Multipath comparison for GPS antenna on GFO mockup.

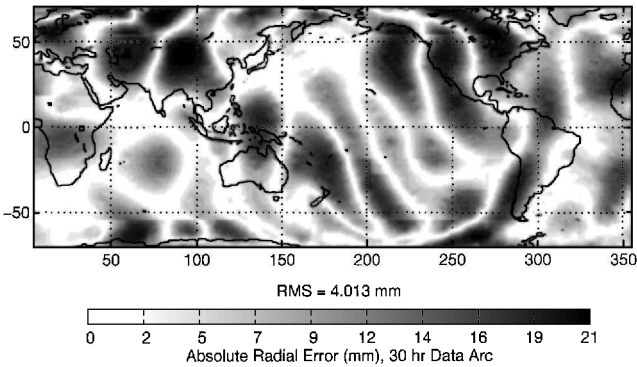


Fig. 5 Total geographically correlated error (10-satellite capable receiver, RDT).

velocity errors of 5 mm/yr were added, as was 1 ms⁻¹ of polar motion error. The combined effect of these error sources is approximately 1.6-cm rms.

Geographically Correlated Errors

Orbit error due to the geopotential exhibits geographic correlation. This correlation is related to the varying geographic distribution of observations used in estimating the gravity field. For example, larger orbit errors generally occur over areas where GPS ground station tracking data is relatively scarce, such as over the Indian and Pacific Oceans. Conversely, smaller errors are present over parts of North America and Europe. Such geographical dependence of orbit accuracy must be minimized to increase the usefulness of the scientific data derived from the altimetry. For certain oceanographic studies, particularly the estimation of global mean sea surfaces, geographically correlated orbit error is problematic because such error will directly affect the results.

An approximation of the geographically correlated orbit error can be derived through knowledge of the covariance of errors in the geopotential coefficients.^{10,11} A set of gravity coefficient error realizations can be generated from the JGM-2 covariance. This random set of correlated coefficient errors can be added to the JGM-2 field to produce a new gravity model having the same statistical correlations as the original. New gravity fields are then used in simulation analysis, just as the TEG-2B field was used before. Global orbit error due to error in the gravity field modeling results from each simulation performed. The geographic correlation of radial orbit error can then be approximated by averaging a sufficiently large number of realizations of the orbit error, 10 for this analysis, and mapping the averaged error to the Earth's surface.

To see how radial orbit errors in the GFO study were correlated with geographic location, contour plots of the absolute value of the averaged error vs latitude and longitude were constructed. A table of the latitude and longitude of the satellite as a function of time was created, and the corresponding radial orbit error and radial velocity were obtained for each position along the GFO groundtrack. A bilinear spatial interpolation scheme, independent of time, was used to process these data to obtain information over single-degree latitude and longitude intervals, a one-by-one-degree grid, for the entire globe. The data were then sorted into ascending or descending passes depending on whether the radial velocity was negative or positive. Because the orbit perigee is maintained at 90 deg, negative vertical velocities correspond to ascending passes. The results from ascending and descending pass geographically correlated orbit errors were averaged separately and then plotted together in Fig. 5. The rms total radial orbit error that can be attributed to geographically correlated error is about 4 mm.

Overall Orbit Accuracy Results

The radial orbit error for GFO obtained by using the RDT and considering all error sources simultaneously, using a 10-satellite capable GPS receiver and six ground stations, was 4.3-cm rms. As expected, the errors associated with the gravity field are dominant. Cases for the five-satellite configuration were also completed for the grouped error sources and yielded 5.5-cm-radial rms error.

Table 4 Radial rms orbit error (cm)

Error source	13 stations		6 stations	
	GFO	T/P	GFO	T/P
Gravity	2.2	0.6	3.4	1.2
Atmospheric drag	1.3	0.4	1.6	0.4
GPS orbits	0.4	0.6	1.2	0.6
Station location	0.4	0.6	0.8	0.4
Others	1.6	1.2	1.6	1.2
Total	3.0	1.6	4.3	1.9

Table 5 Radial rms orbit accuracy (cm): dynamic technique and RDT

Orbit determination technique	Radial accuracy, cm
Dynamic (moderate drag)	7.8
Dynamic (high drag)	11.6
RDT (moderate drag)	4.2
RDT (high drag)	4.3

Table 6 Effect of tuning the RDT sigma (radial error, cm)

Sigma, nm/s ²	13 stations	
	GEOSAT	T/P
1	3.6	2.3
10	3.0	1.6
50	3.1	1.6
100	3.1	1.7
1000	3.0	1.7

Table 4 contains the radial accuracy by error component for both the GEOSAT and T/P orbits. These results are for an RDT steady-state sigma of 10 nm/s². The results show that increasing the number of ground stations to 13 reduces the radial error to 3.0-cm rms in the GEOSAT orbit and from 1.9 to 1.6 cm rms in the T/P orbit. In each orbit, gravity remains the largest error contributor, but errors can be reduced by using more stations and tuning of model parameters, such as gravity field coefficients.

The orbit accuracy is determined by differencing the orbit used to generate the data set with that obtained from filtering and smoothing. The differences are taken in Cartesian coordinates and then rotated to a local spacecraft radial, cross, and along-track coordinate system. Table 5 gives a comparison of the radial orbit accuracy using dynamic and reduced dynamic orbit determination techniques. A 10-satellite-capable receiver was assumed, although the dynamic results are relatively insensitive to the number of channels. The dynamic analysis estimated only the drag coefficient, once-per-revolution radial sinusoidal acceleration, and solar radiation parameters. All results in Table 5 were completed assuming a six-station tracking configuration.

GPS measurements from ground tracking stations are an important part of the orbit determination procedure. Ground-based measurements allow the estimation of GPS-related clock and orbit errors, as well as removal of selective availability corruption of the data. In earlier work, six ground stations were assumed in the simulation mode.¹² Currently, 13–16 stations are typically used by JPL in the daily T/P solutions. By including a larger number of ground stations, more information is available for correcting the orbits and clocks. Including more measurements is especially important for reduced dynamic solutions considering the extra parameters that must be estimated at each epoch of interest. The expected result of more stations is that the orbit determination accuracy should improve. As Table 4 illustrates, the result of increasing the station number from 6 to 13 is orbit accuracy improvement. The result is particularly dramatic in the GEOSAT orbit, which has a higher drag and gravity error influence.

The results of tuning the RDT parameter are given in Table 6 for five values of the steady-state sigma. The results show that optimally tuning sigmas for the RDT can also reduce the overall radial orbit error.

Conclusions

Simulation analysis completed with JPL's GIPSY-OASIS II software, using conservative assumptions, shows that a radial orbit accuracy of 4.3 cm can be obtained in the GEOSAT exact repeat orbit using a 10-satellite-capable GPS receiver. Results show that increasing the number of stations from 6 to 13 reduces the error to 3.0-cm rms in the GEOSAT orbit and from 1.9- to 1.6-cm rms in the T/P orbit. The gravity error is the largest contributor. In addition, tuning the reduced dynamic tracking steady-state sigma for a given configuration also reduces the orbit determination error.

After this study was completed, the decision was made to use a Turbo-Star eight-channel receiver for the GFO mission. The resulting accuracy with this receiver should be comparable to that for the 10-satellite-capable receiver in this study. In the GFO orbit, generally a maximum of 8 satellites are visible, with occasionally 9 or 10 visible for short periods of time. These few extra observations will not substantially change the attainable orbit accuracy.

Gravity field improvement for the GEOSAT orbit has been under investigation at the University of Texas, where it was shown that the gravity model could be improved by using GPS tracking data from less than one repeat period of the first GFO satellite during solar minimum activity.¹² This study indicated that the rms radial orbit error using dynamic orbit determination decreased by 45% (from 8.2 to 4.5 cm) as a direct result of geopotential model tuning. Applied to the RDT technique, tuning should reduce radial error due to gravity mismodeling by a similar factor (perhaps from 3.4 to 1.9 cm for the six-station configuration).

Acknowledgments

This analysis was supported in part by contracts from the U.S. Naval Research Laboratory, by NASA Langley Grant NAG-1-1941, and a Ball Aerospace contract. Willy Bertiger and George Hajj at the Jet Propulsion Laboratory provided support and technical advice for this analysis. Peter MacDoran and Charles Behre at CU and Skip Cubbedge at Ball Aerospace performed the setup and analysis of the multipath mockup experiment. Patrick Binning and Robert Markin at CU performed some of the early simulation analysis, and William Frazier and Scott Mitchell from Ball Aerospace provided support and technical advice for the paper.

References

¹Muellerschoen, R. J., Lichten, S. L., Lindqwister, U. J., and Bertiger, W. I., "Results of an Automate GPS Tracking System in Support of

Topex/Poseidon and GPSMet," Inst. of Navigation GPS-95 International Meeting, ION Paper 95107, Palm Springs, CA, Sept. 1995.

²Tapley, B. D., Ries, J. C., Davis, G. W., Eanes, R. J., Schutz, B. E., Schum, C. K., Watkins, M. M., Marshall, J. A., Nerem, R. S., Putney, B. H., Klosko, S. M., Luthcke, S. B., Pavlis, D., Williamson, R. G., and Zelensky, N. P., "Precision Orbit Determination for TOPEX/POSEIDON," *Journal of Geophysical Research*, Vol. 99, No. 12, 1994, pp. 24,383-24,389.

³Lichten, S. M., Bar-Sever, Y. E., Bertiger, W. I., Heflin, M., Hurst, K., Muellerschoen, R. J., Wu, S. C., Yunck, T. P., and Zumberge, J., "GIPSY-OASIS II: A High Precision GPS Data Processing System and General Satellite Orbit Analysis Tool," *Technology 2005*, NASA Technology Transfer Conf., Rept. 95-1037, Chicago, IL, Oct. 1995.

⁴Zumberge, J. F., Heflin, M. B., Jefferson, D. C., Watkins, M. M., and Webb, F. H., "Jet Propulsion Laboratory IGS Analysis Center 1994 Annual Report," *International GPS Service for Geodynamics 1994 Annual Report*, edited by J. F. Zumberge, R. Liu, and R. E. Neilan, Jet Propulsion Lab., California Inst. of Technology, Pasadena, CA, 1995, pp. 30-39.

⁵Tapley, B. D., Ries, J. C., and Zelensky, N. P., "Precision Orbit Determination for TOPEX/POSEIDON," *Journal of Geophysical Research Letters*, Vol. 21, No. 19, 1994, p. 2438.

⁶Wu, S. C., Yunck, T. P., and Thornton, C. L., "Reduced-Dynamic Technique for Precise Orbit Determination for Low Earth Satellites," AAS/AIAA Astrodynamics Specialist Conf., American Astronautical Society, AAS Paper 87-410, Kalispell, MT, Aug. 1987.

⁷Davis, G. W., "GPS-Based Precision Orbit Determination for Low Altitude Geodetic Satellites," Ph.D. Dissertation, Dept. of Aerospace Engineering, Univ. of Texas, Austin, TX, May 1996.

⁸Hedin, A. E., and Mayr, H. G., "Characteristics of Wavelike Fluctuations in Dynamics Explorer Neutral Composition Data," *Journal of Geophysical Research*, Vol. 92, No. A10, 1987, pp. 11,159-11,172.

⁹Hajj, G. A., "The Multipath Simulator, A Tool Toward Controlling Multipath," Second Symposium on GPS Applications in Space, Hanscom AFB, MA, Feb. 1990.

¹⁰Mitchell, S., "A Study of Geographically Correlated Orbit Errors for TOPEX—Incorporating GPS Data," Ph.D. Dissertation, Colorado Center for Astrodynamics Research, Univ. of Colorado, Boulder, CO, Dec. 1990.

¹¹Rosborough, G. W., and Mitchell, S., "Geographically Correlated Orbit Error for the TOPEX Satellite Using GPS Tracking," AIAA Paper 90-2956, Aug. 1990.

¹²Davis, G. W., Rim, H. J., Ries, J. C., and Tapley, B. D., "Tracking System Options for Future Altimeter Satellite Missions," Univ. of Texas Center for Space Research, Rept. 94-0142, Austin, TX, Aug. 1994.

F. H. Lutze Jr.
Associate Editor